

Numerical investigation of electromagnetic wave propagation generated by localized sources using a high order discontinuous Galerkin time domain method

Daniel Gieschen

NACHOS project-team of INRIA, Sophia Antipolis

University of Nice

July 2009

Outline

- 1 Theoretical part
 - Maxwell equations
 - Numerical Scheme
 - Source Term
- 2 Numerical Study
 - Propagation in free space
 - Propagation involving a room
 - Propagation involving objects inside the room

Introducing the topics of the internship

Maxwell equations

Numerical investigation of *electromagnetic wave propagation* generated by localized sources using a high order discontinuous Galerkin time domain method

Introducing the topics of the internship

Numerical Scheme

Numerical investigation of electromagnetic wave propagation generated by localized sources ***using a high order discontinuous Galerkin time domain method***

Introducing the topics of the internship

Source term

Numerical investigation of electromagnetic wave propagation
generated by localized sources using a high order discontinuous
Galerkin time domain method

Outline

- 1 Theoretical part
 - Maxwell equations
 - Numerical Scheme
 - Source Term
- 2 Numerical Study
 - Propagation in free space
 - Propagation involving a room
 - Propagation involving objects inside the room

Definition of the Maxwell equations in n dimensions

Definition

$$\nabla \cdot \mathbf{E} = 0$$

$$\nabla \cdot \mathbf{B} = 0$$

$$\varepsilon \frac{\partial \mathbf{E}}{\partial t} = \text{rot } \mathbf{H}$$

$$\mu \frac{\partial \mathbf{H}}{\partial t} = -\text{rot } \mathbf{E}$$

Definition of the Maxwell equations in two dimensions

Definition

On a bounded domain $\Omega \subset \mathbb{R}^2$

$$\varepsilon \frac{\partial E_z}{\partial t} - \frac{\partial H_y}{\partial x} + \frac{\partial H_x}{\partial y} = 0,$$

$$\mu \frac{\partial H_x}{\partial t} + \frac{\partial E_z}{\partial y} = 0,$$

$$\mu \frac{\partial H_y}{\partial t} - \frac{\partial E_z}{\partial x} = 0,$$

Variables

- Magnetic field \mathbf{H}
- Electric field \mathbf{E}
- Electric permittivity ε
- Magnetic permeability μ

First order Silver-Müller absorbing boundary condition

Definition

On the boundary of the domain $\Gamma = \partial\Omega$

$$E_z = c\mu(n_y H_x - n_x H_y)$$

where $c = 1/\sqrt{\epsilon\mu}$ and $\vec{n} = (n_x, n_y)$

Variables

- Speed of propagation c
- Unit outer normal vector \vec{n}

Outline

- 1 Theoretical part
 - Maxwell equations
 - **Numerical Scheme**
 - Source Term

- 2 Numerical Study
 - Propagation in free space
 - Propagation involving a room
 - Propagation involving objects inside the room

Considering a partition \mathcal{T}_h of Ω

Definitions

- Triangles T_i are of size h_i with boundaries ∂T_i and characteristic mesh size $h = \max_{T_i \in \mathcal{T}_h} h_i$.
- Seek for an approximate solution in the finite dimensional subspace $V_p(\mathcal{T}_h)$
- $V_p(\mathcal{T}_h) := \{v \in L^2(\Omega) : v|_{T_i} \in \mathbb{P}_p(T_i), \forall T_i \in \mathcal{T}_h\}$
- $\mathbb{P}_p(T_i)$ is the space of nodal polynomials $\{\varphi_{ij}\}_{j=1}^d$ of total degree at most p
- For neighboring triangles T_i and T_k the intersection $T_i \cap T_k$ is an edge s_{ik} , called interface.

Spatial discretization of the equations.

$$\int_{T_i} \varepsilon_i \frac{\partial E_z}{\partial t} \varphi_{ij} + \int_{T_i} H_y \frac{\partial \varphi_{ij}}{\partial x} - \int_{T_i} H_x \frac{\partial \varphi_{ij}}{\partial y} - \int_{\partial T_i} H_y \varphi_{ij} \tilde{n}_{ikx} + \int_{\partial T_i} H_x \varphi_{ij} \tilde{n}_{iky} = 0,$$

$$\int_{T_i} \mu_i \frac{\partial H_x}{\partial t} \varphi_{ij} - \int_{T_i} E_z \frac{\partial \varphi_{ij}}{\partial y} + \int_{\partial T_i} E_z \varphi_{ij} \tilde{n}_{iky} = 0,$$

$$\int_{T_i} \mu_i \frac{\partial H_y}{\partial t} \varphi_{ij} + \int_{T_i} E_z \frac{\partial \varphi_{ij}}{\partial x} - \int_{\partial T_i} E_z \varphi_{ij} \tilde{n}_{ikx} = 0.$$

Time discretization with leap-frog scheme

- Δt is the fixed time-step
- $\mathbf{E}_{z_i}^n$ are approximated at integer time stations $t^n = n\Delta t$
- $\mathbf{H}_{x_i}^{n+\frac{1}{2}}$ and $\mathbf{H}_{y_i}^{n+\frac{1}{2}}$ are approximated at half-integer time stations $t^{n+\frac{1}{2}} = (n + \frac{1}{2})\Delta t$
- An absorbing boundary interface s_{ik} is defined by $\forall (x, y) \in s_{ik} : \mathbf{E}_{z_k}^{n+1}(x, y) = c_i \mu_i (n_{iky} \mathbf{H}_{x_i}^{n+\frac{1}{2}}(x, y) - n_{ikx} \mathbf{H}_{y_i}^{n+\frac{1}{2}}(x, y))$.

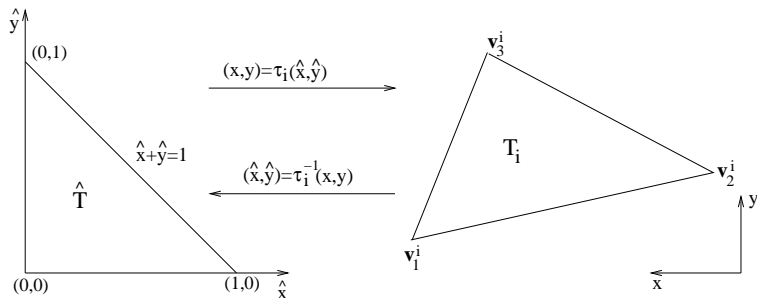
The discontinuous Galerkin DGTD- \mathbb{P}_p method in matrix form,

$$\begin{aligned} \mathbb{M}_i^\varepsilon \frac{\mathbf{E}_{z_i}^{n+1} - \mathbf{E}_{z_i}^n}{\Delta t} &= -\mathbb{K}_i^x \mathbf{H}_{y_i}^{n+\frac{1}{2}} + \mathbb{K}_i^y \mathbf{H}_{x_i}^{n+\frac{1}{2}} \\ &\quad + \sum_{k \in \mathcal{V}_i} (\mathbb{G}_{x_{ik}}^{n+\frac{1}{2}} - \mathbb{G}_{y_{ik}}^{n+\frac{1}{2}}), \\ \mathbb{M}_i^\mu \frac{\mathbf{H}_{x_i}^{n+\frac{1}{2}} - \mathbf{H}_{x_i}^{n-\frac{1}{2}}}{\Delta t} &= \mathbb{K}_i^y \mathbf{E}_{z_i}^n - \sum_{k \in \mathcal{V}_i} \mathbb{F}_{y_{ik}}^n, \\ \mathbb{M}_i^\mu \frac{\mathbf{H}_{y_i}^{n+\frac{1}{2}} - \mathbf{H}_{y_i}^{n-\frac{1}{2}}}{\Delta t} &= -\mathbb{K}_i^x \mathbf{E}_{z_i}^n + \sum_{k \in \mathcal{V}_i} \mathbb{F}_{x_{ik}}^n, \end{aligned}$$

with the following vector and matrix quantities.

$$\left\{ \begin{array}{ll} \mathbf{F}_{x_{ik}}^n = \mathbf{S}_{ik}^x \mathbf{E}_{z_k}^n & , \quad \mathbf{F}_{y_{ik}}^n = \mathbf{S}_{ik}^y \mathbf{E}_{z_k}^n, \\ \mathbf{G}_{x_{ik}}^{n+\frac{1}{2}} = \mathbf{S}_{ik}^x \mathbf{H}_{y_k}^{n+\frac{1}{2}} & , \quad \mathbf{G}_{y_{ik}}^{n+\frac{1}{2}} = \mathbf{S}_{ik}^y \mathbf{H}_{x_k}^{n+\frac{1}{2}}, \\ (\mathbf{M}_i^\varepsilon)_{jl} = \int_{T_i} \varepsilon_i \varphi_{ij} \varphi_{il} & , \quad (\mathbf{M}_i^\mu)_{jl} = \int_{T_i} \mu_i \varphi_{ij} \varphi_{il}, \\ (\mathbf{K}_i^x)_{jl} = \frac{1}{2} \int_{T_i} \left(\frac{\partial \varphi_{ij}}{\partial x} \varphi_{il} - \varphi_{ij} \frac{\partial \varphi_{il}}{\partial x} \right) & , \quad (\mathbf{S}_{ik}^x)_{jl} = \frac{1}{2} \tilde{n}_{ikx} \int_{s_{ik}} \varphi_{ij} \varphi_{kl}. \end{array} \right.$$

Mapping between the physical triangle T_i and the master triangle \hat{T} .



The fixed reference triangle $\hat{T} = \{\hat{x}, \hat{y} \mid \hat{x}, \hat{y} \geq 0; \hat{x} + \hat{y} \leq 1\}$ has a smooth bijective mapping τ_i to each triangle T_i of the mesh.

Outline

- 1 Theoretical part
 - Maxwell equations
 - Numerical Scheme
 - Source Term
- 2 Numerical Study
 - Propagation in free space
 - Propagation involving a room
 - Propagation involving objects inside the room

Source term in z-direction

$$\varepsilon \frac{\partial E_z}{\partial t} - \frac{\partial H_y}{\partial x} + \frac{\partial H_x}{\partial y} = -J_z(x, y, t)$$

where the radiating source $J_z(x, y, t)$ is of

Dirac type

$$f(t)\delta(x - x_0, y - y_0)$$

$$\delta(x, y) = \begin{cases} 1 & \text{if } x, y = 0, \\ 0 & \text{elsewhere.} \end{cases}$$

Gaussian type

$$f(t)g(x, y)$$

$$g(x, y) = Ae^{-((x-x_0)^2 + (y-y_0)^2)}$$

Leads to the discrete equation for E_z

$$M_i^\varepsilon \frac{E_{z_i}^{n+1} - E_{z_i}^n}{\Delta t} = -K_i^x H_{y_i}^{n+\frac{1}{2}} + K_i^y H_{x_i}^{n+\frac{1}{2}} + \sum_{k \in \mathcal{V}_i} (G_{x_{ik}}^{n+\frac{1}{2}} - G_{y_{ik}}^{n+\frac{1}{2}})$$

Dirac type

$$-f(t)\varphi_{ij}(x_0, y_0)$$

Gaussian type

$$-f(t) \sum_j g(x_j - x_0, y_j - y_0) \int_{T_i} \varphi_{ij} \varphi_{il}$$

Outline

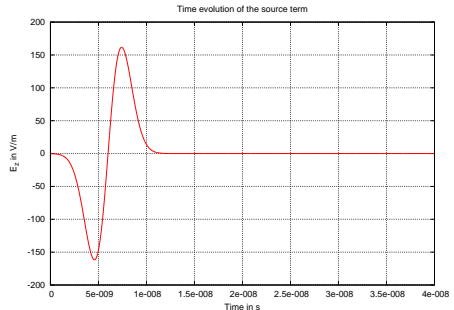
- 1 Theoretical part
 - Maxwell equations
 - Numerical Scheme
 - Source Term
- 2 Numerical Study
 - Propagation in free space
 - Propagation involving a room
 - Propagation involving objects inside the room

The problem statement (in general)

- Numerical methodology for designing a radar-based imaging system.
- Considering simulation setting of increasing complexity.
- Record the propagation patterns.

The problem statement (in practise)

- First order Silver-Müller absorbing boundary condition.
- Radiating source.
- Visualization points.
- Numerical assessment of the accuracy and reflection.

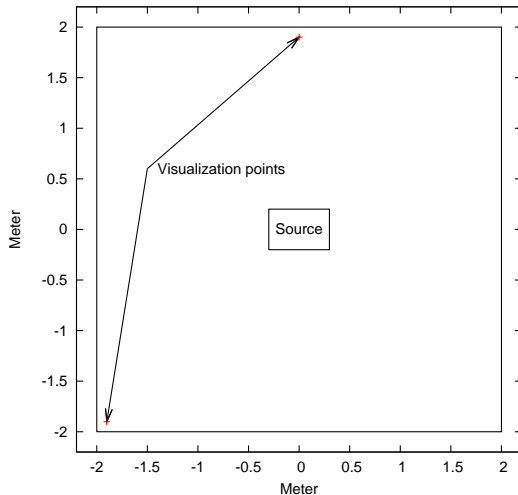


Outline

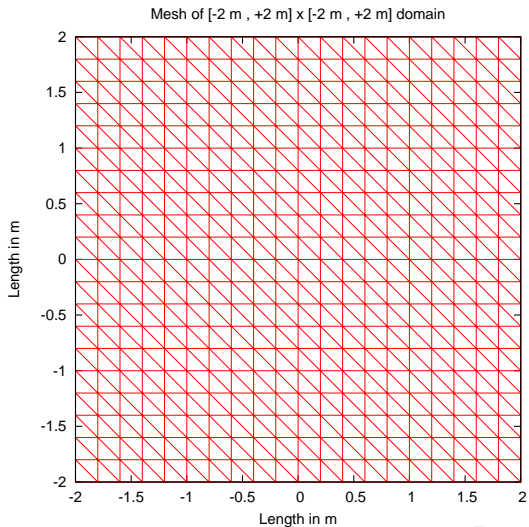
- 1 Theoretical part
 - Maxwell equations
 - Numerical Scheme
 - Source Term
- 2 Numerical Study
 - Propagation in free space
 - Propagation involving a room
 - Propagation involving objects inside the room

The simulation settings

Sample plot of the domain and its visualization points



The simulation settings (mesh)



Main results of the observation

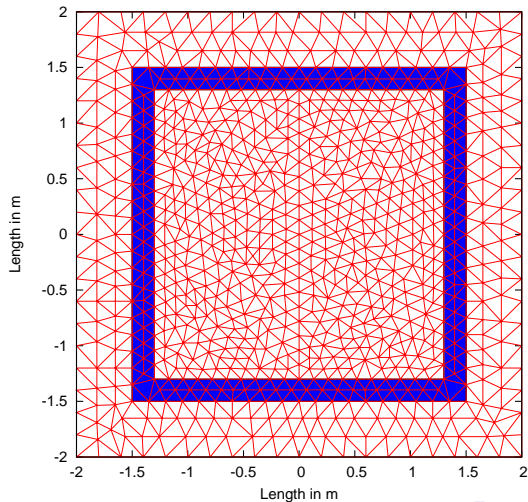
- Both visualization points show very similar propagation patterns
- Increasing the mesh resolution show there is very small artificial reflections at the absorbing boundary, 1% at $t = 50 \text{ ns}$ in the worst case
- A higher order of the DGTD- \mathbb{P}_p method leads to a more accurate solution, but for the Dirac source type for $t \geq 10 \text{ ns}$
- For different sized domains we observe a time shift and different absolute values of the amplitudes. There is more noise in larger domains.
- In the energy analysis we observe that for the Dirac source type the DGTD- \mathbb{P}_2 method converges to zero the fastest, Gaussian source type leads to faster convergence.

Outline

- 1 Theoretical part
 - Maxwell equations
 - Numerical Scheme
 - Source Term
- 2 Numerical Study
 - Propagation in free space
 - **Propagation involving a room**
 - Propagation involving objects inside the room

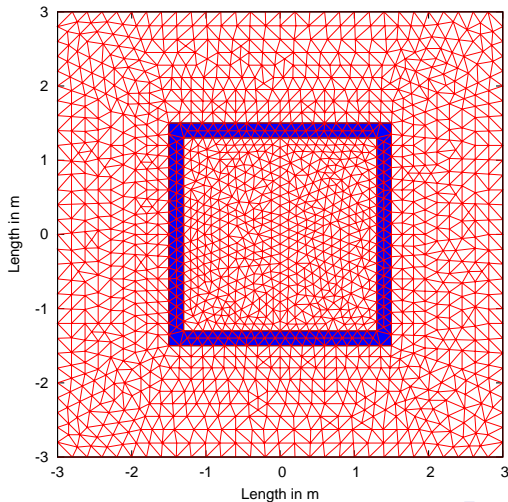
The simulation settings

Mesh of $[-2\text{ m}, +2\text{ m}] \times [-2\text{ m}, +2\text{ m}]$ domain with wall (about 1000 vertices)



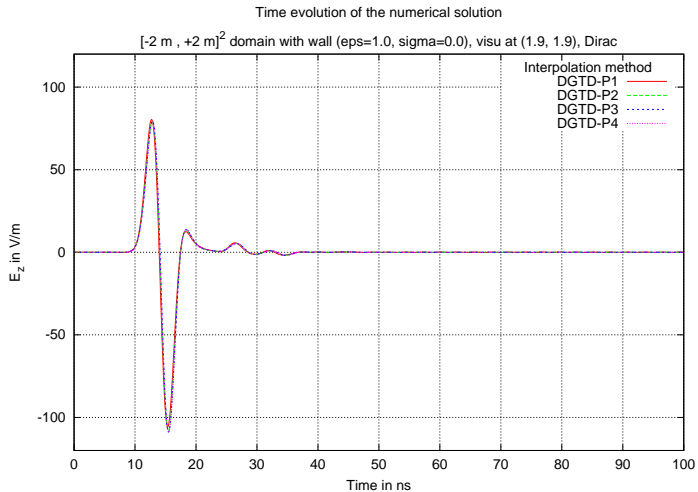
The simulation settings

Mesh of $[-3 \text{ m}, +3 \text{ m}] \times [-3 \text{ m}, +3 \text{ m}]$ domain with wall (about 1700 vertices)



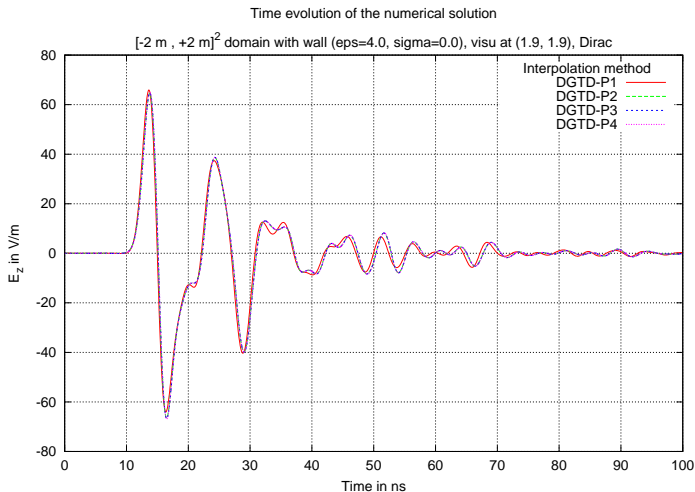
Influence of the electrical permittivity ε and conductivity σ

$\varepsilon = 1$ and $\sigma = 0$



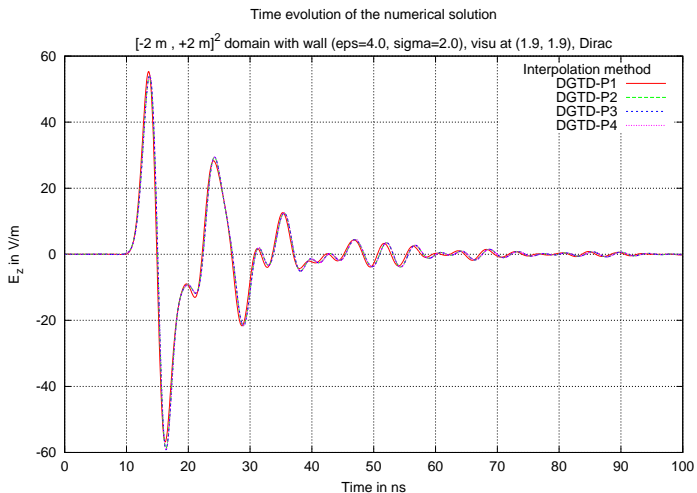
Influence of the electrical permittivity ϵ and conductivity σ

$\epsilon = 4$ and $\sigma = 0$



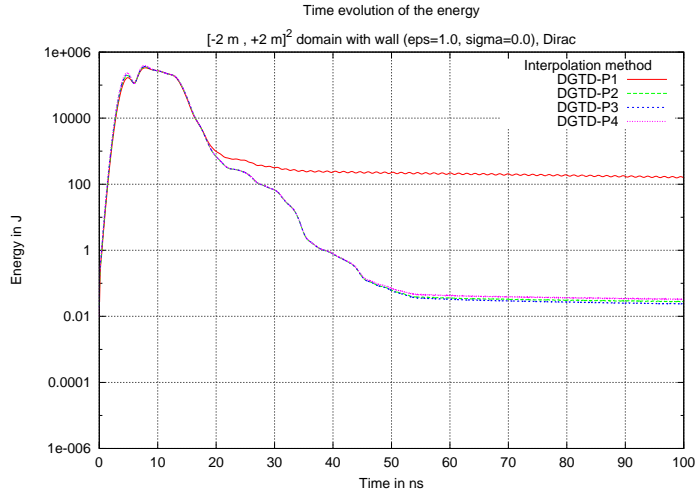
Influence of the electrical permittivity ϵ and conductivity σ

$\epsilon = 4$ and $\sigma = 2$



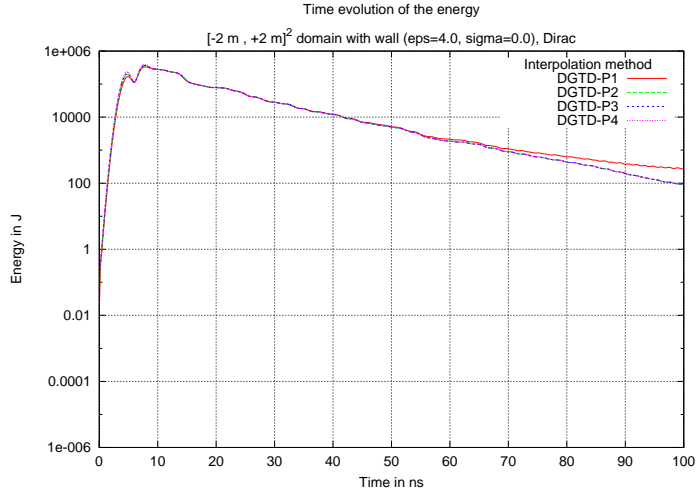
Influence of the electrical permittivity ϵ and conductivity σ

$\epsilon = 1$ and $\sigma = 0$



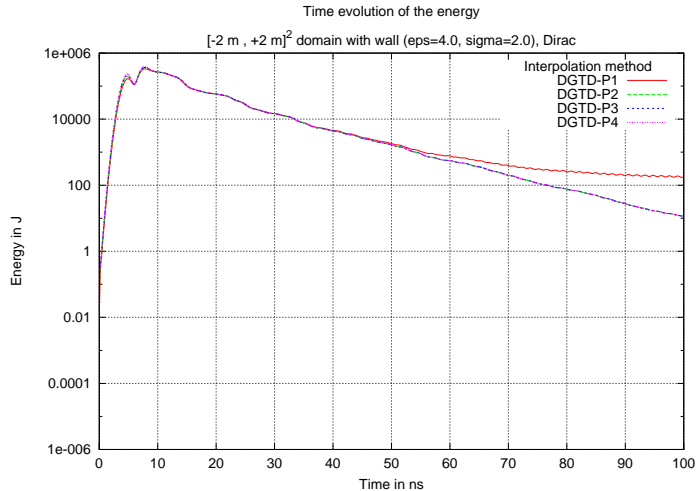
Influence of the electrical permittivity ε and conductivity σ

$\varepsilon = 4$ and $\sigma = 0$



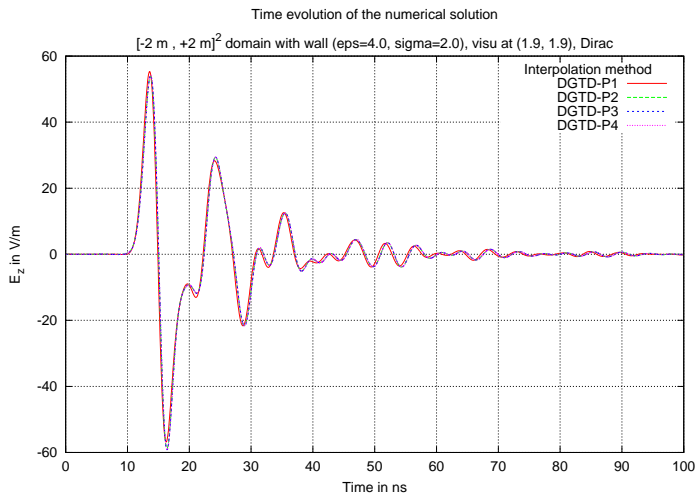
Influence of the electrical permittivity ε and conductivity σ

$\varepsilon = 4$ and $\sigma = 2$



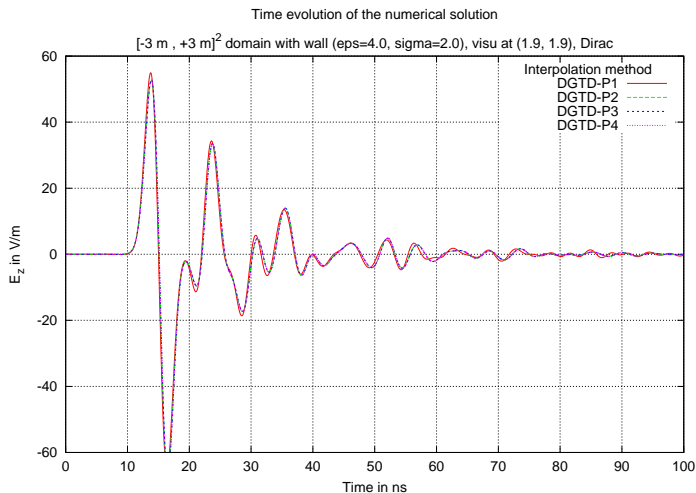
Influence of the size of the computational domain

A $[-2\text{ m}, +2\text{ m}]^2$ domain, visualization point $A = (1.9, 1.9)$



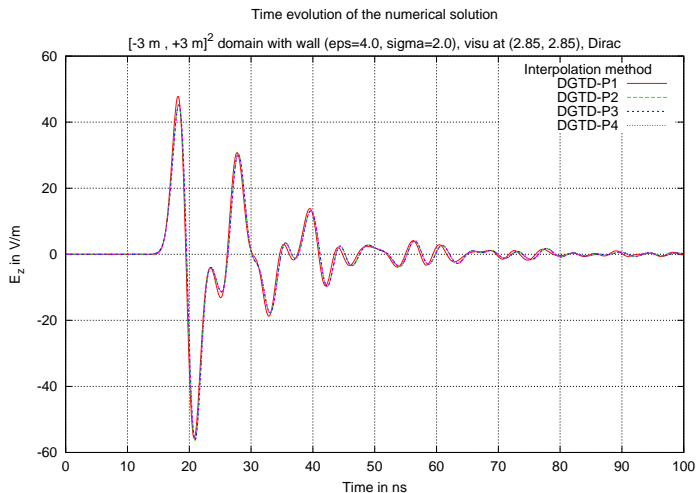
Influence of the size of the computational domain

A $[-3\text{ m}, +3\text{ m}]^2$ domain, visualization point $A = (1.9, 1.9)$



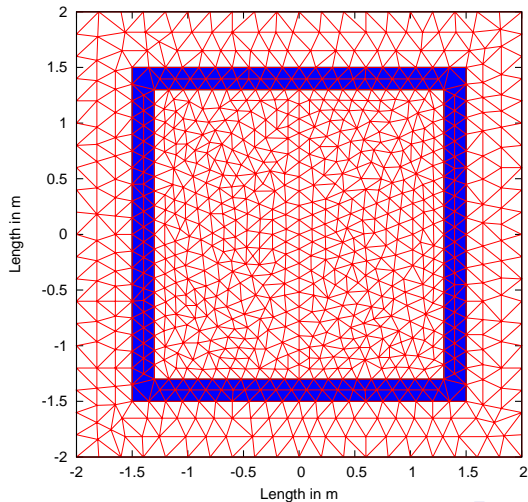
Influence of the size of the computational domain

A $[-3\text{ m}, +3\text{ m}]^2$ domain, visualization point $B = (2.85, 2.85)$



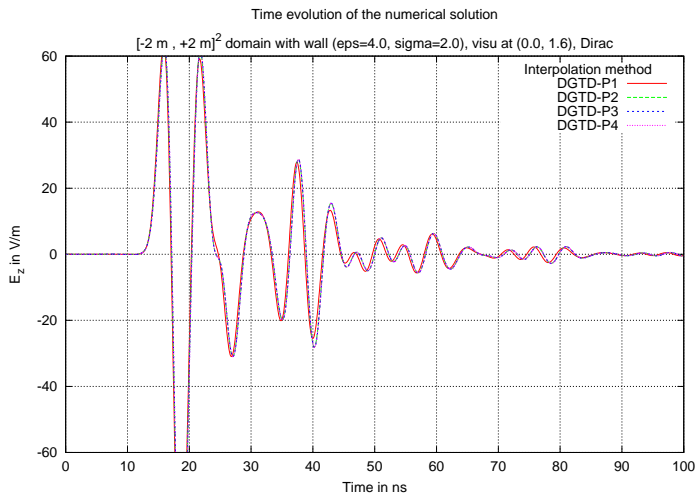
The simulation settings

Mesh of $[-2 \text{ m}, +2 \text{ m}] \times [-2 \text{ m}, +2 \text{ m}]$ domain with wall (about 1000 vertices)



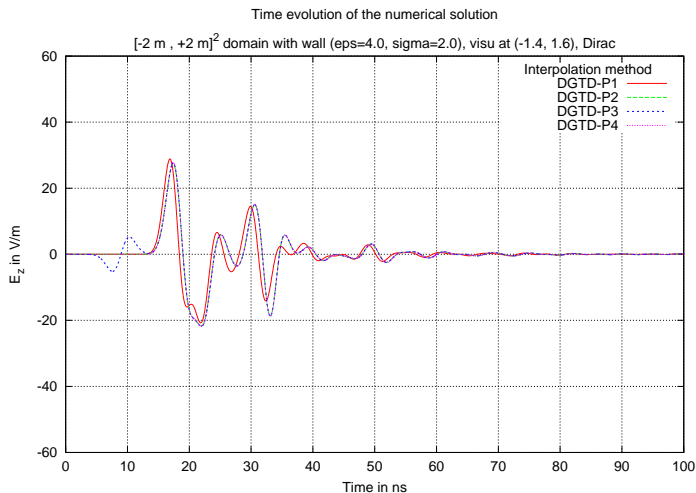
Influence of the position of the source

Top center visualization point



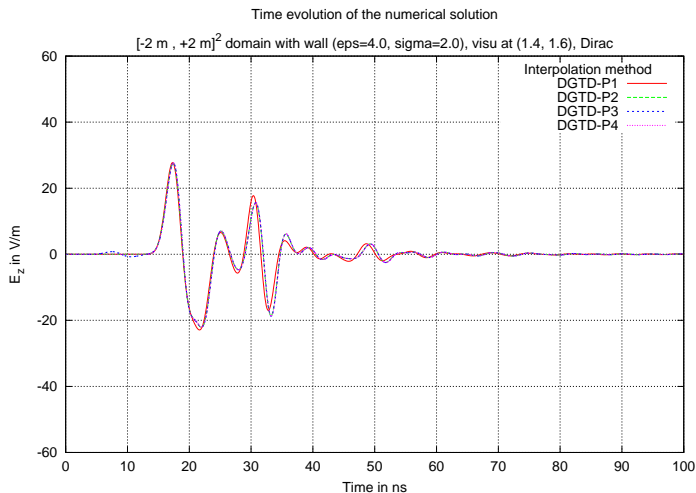
Influence of the position of the source

Top left visualization point



Influence of the position of the source

Top right visualization point

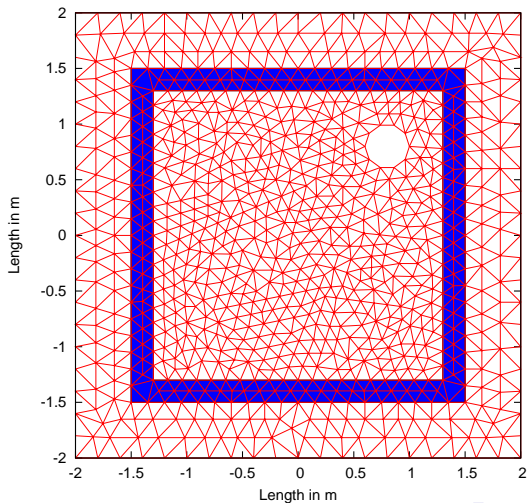


Outline

- 1 Theoretical part
 - Maxwell equations
 - Numerical Scheme
 - Source Term
- 2 Numerical Study
 - Propagation in free space
 - Propagation involving a room
 - Propagation involving objects inside the room

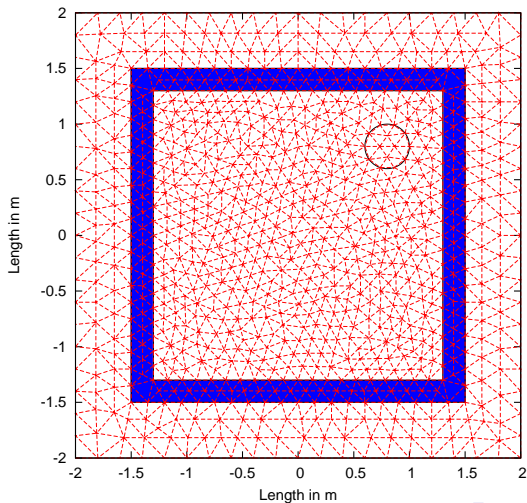
The simulation settings

Mesh of $[-2\text{ m}, +2\text{ m}] \times [-2\text{ m}, +2\text{ m}]$ domain with wall and metallic object (about 1000 vertices)



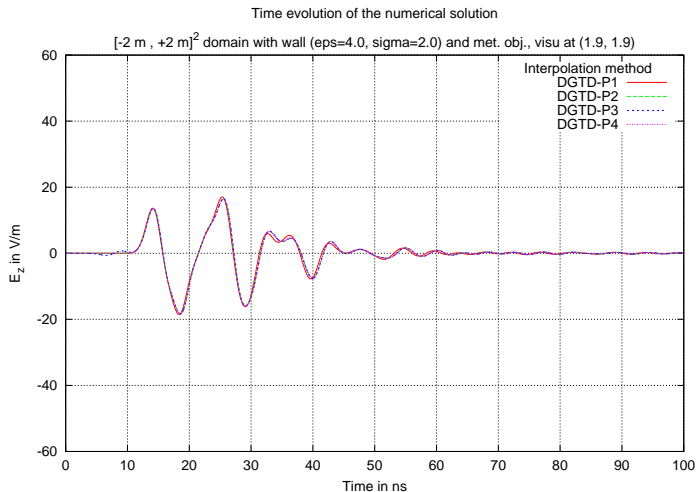
The simulation settings

Mesh of $[-2 \text{ m}, +2 \text{ m}] \times [-2 \text{ m}, +2 \text{ m}]$ domain with wall and metallic object (about 1000 vertices)



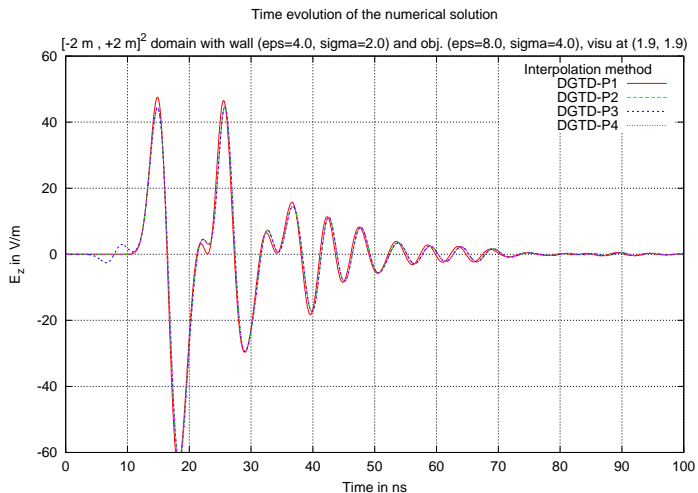
Influence of the type of object inside the room

Metallic object



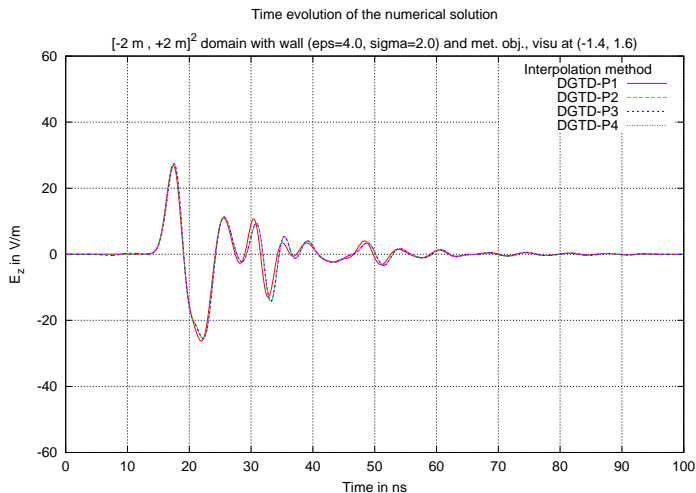
Influence of the type of object inside the room

Meshed object with $\epsilon = 8$ and $\sigma = 4$



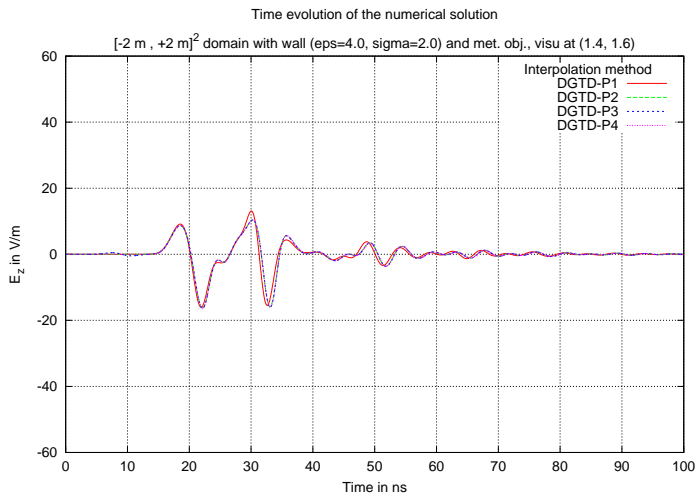
Influence of the position of the source

Top left visualization point, metallic object



Influence of the position of the source

Top right visualization point, metallic object



Summary and conclusions

- The introduction of **discontinuous Galerkin time domain method** for the **two-dimensional Maxwell equations** with a radiating source term.
- The numerical analysis of **propagation patterns for different scenarios** with increasing complexity.
- Outlook
 - We established a basis for further investigation in an efficient good structured way.
 - Investigations for real physical quantities, more complex scenarios and in more detail.
 - Development of a radar-based imaging system.

Summary and conclusions

Thank you for listening!